Table S1. Blank correction for size-fractionated particles. POC = particulate organic carbon, QMA = quartz microfiber filter, Ag = silver filter.

Parameter	Units	Filter type	Fraction analyzed (%)	Size class (µm)	Average ± standard deviation	% Average contribution to samples
POC	µmol C	QMA (142 mm)	3.4	1–51	3.5 ± 0.5 (n = 8)	13.8
Thorium-234	dpm	QMA (142 mm)	3.4	1–51	0.07 ± 0.06 (n = 8)	1.8
POC	µmol C	Ag (25 mm)	50-100	51–335, >335	1.4 ± 0.5 (n = 15)	5.3
Thorium-234	dpm	Ag (25 mm)	100	51–335, >335	0.06 ± 0.04 (n = 16)	2.3
Biogenic silica	µmol Si	Ag (25 mm)	50-100	51–335, >335	0.23 ± 0.18 (n = 7)	6.4

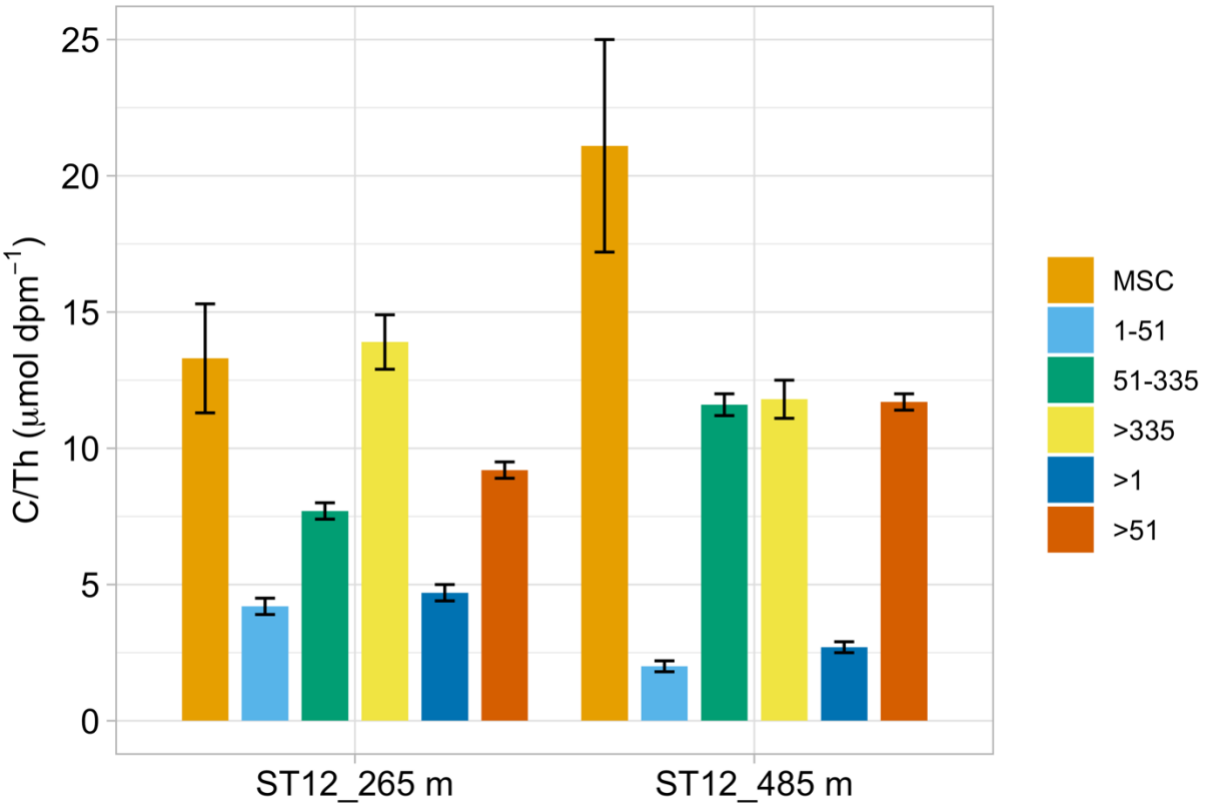

Fig. S1. Comparison of POC/^{234}Th (C/Th) ratios at Station 12 at two depths (265, 485 m) in sinking particles collected using marine snow catchers (MSC) and in different particle size fractions (1–51, 51–335, >335, >1, >51 µm) collected using large volume pumps.

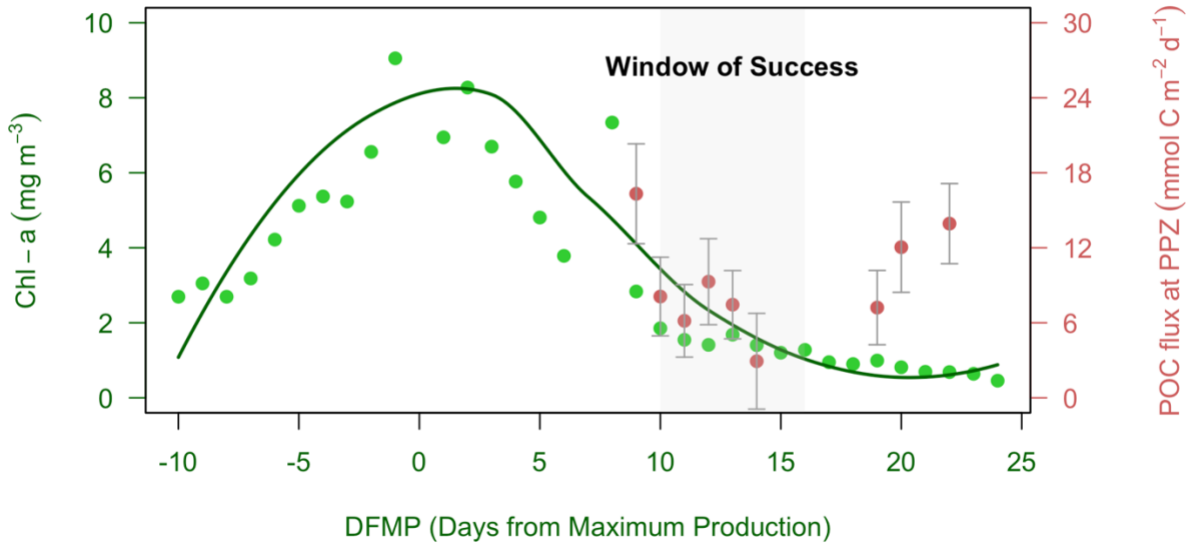

Fig. S2. Trends in satellite-derived chlorophyll-a (chl-a) concentration (Devred et al., 2025) in the Eastern Grid area over time, shown alongside particulate organic carbon (POC) fluxes at the base of the primary production zone (PPZ). DFMP (days from maximum production) = 0 corresponds to the peak of the bloom, when chl-a concentration reached its maximum. The window of success (Ceballos-Romero et al., 2018) is shown with grey shading (see Sect. 2.5).

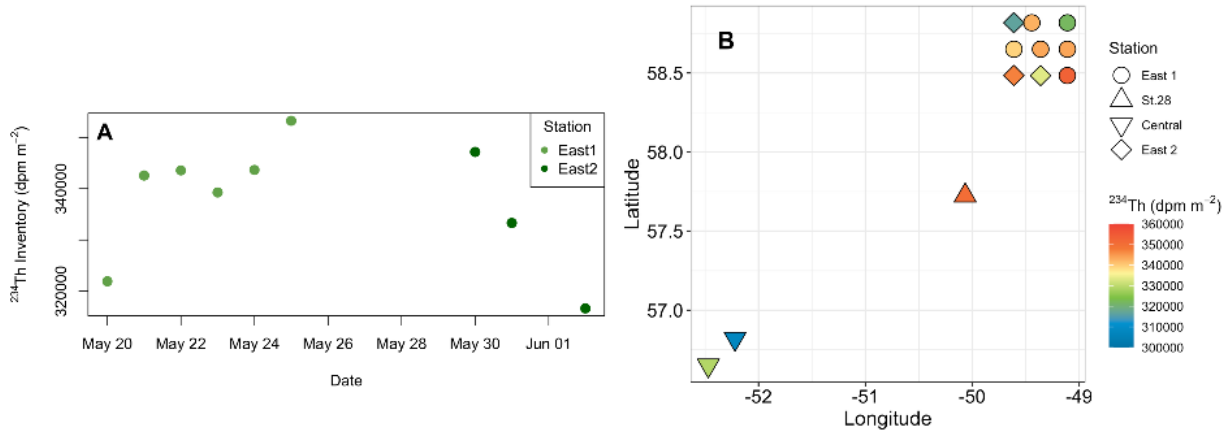

Fig. S3. ^{234}Th inventories in the upper 150 m of the water column in the Eastern Grid vs. time (A) and across all stations sampled during the BELAS-1 expedition (B).

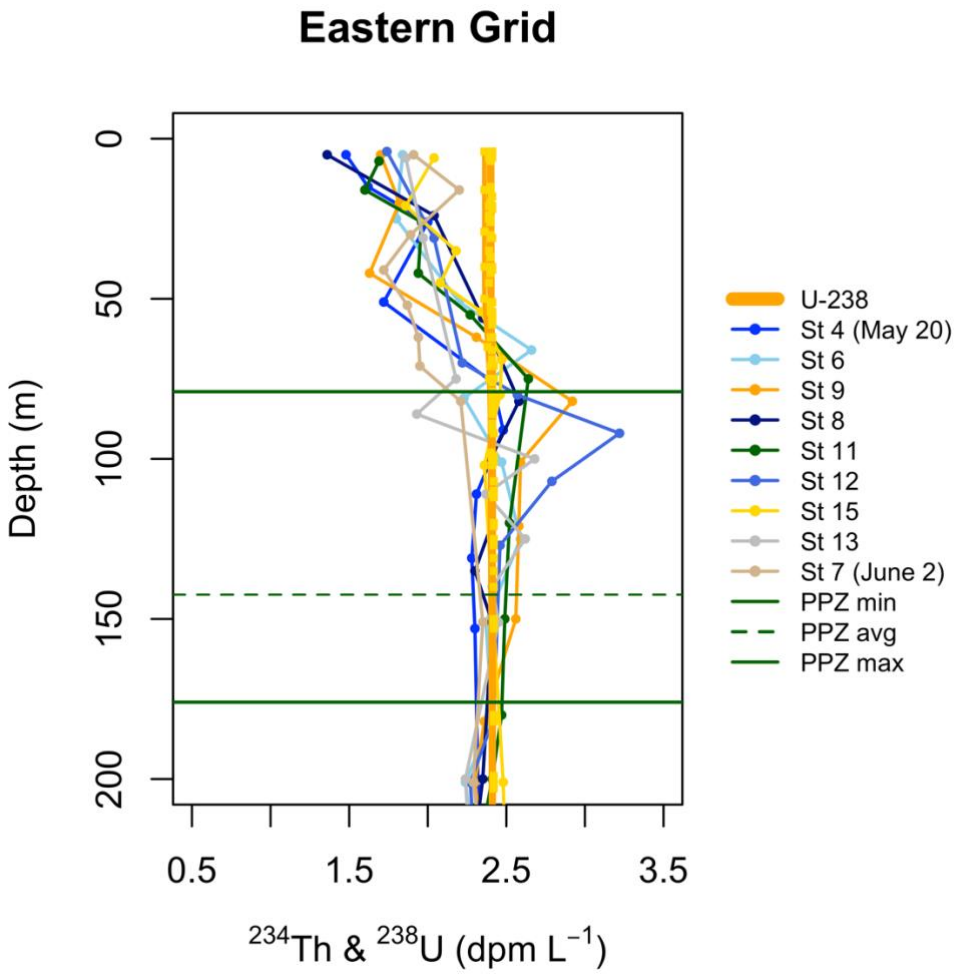

Fig. S4. Profiles of total ^{234}Th and ^{238}U in the upper 200 m of the water column in the Eastern Grid. The base of the primary production zone (PPZ) is shown with green lines (dashed line indicates the average, solid lines indicate the minimum and maximum).

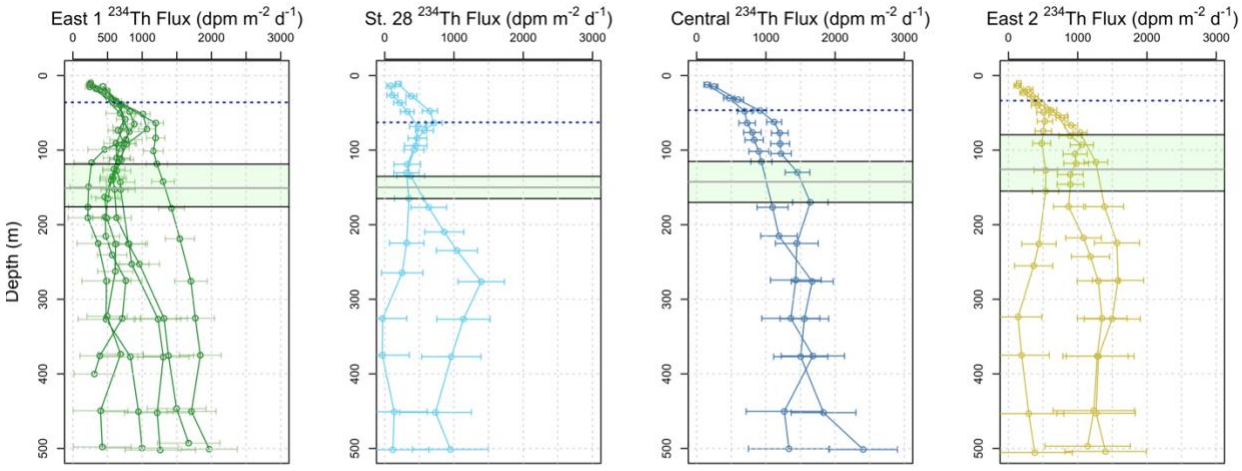

Fig. S5. Profiles of steady state ^{234}Th flux across regions. The base of the primary production zone is shown with green shading (grey solid line indicates the average, black solid lines indicate the minimum and maximum) and the average base of the mixed layer is shown with a blue dashed line.

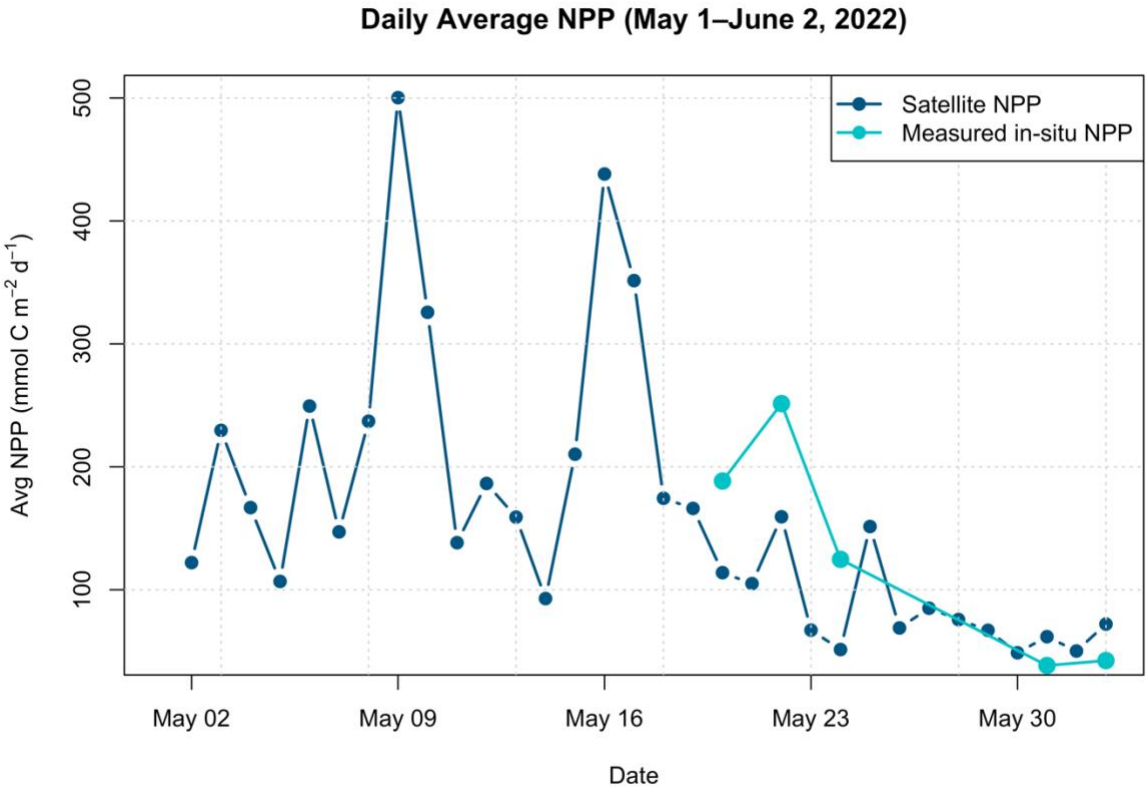

Fig. S6. Satellite net primary production (NPP) and measured in situ NPP in the Eastern Grid area from 2 May to 2 June 2022. Satellite NPP data was supplied by the Satellite Ocean colour and Phytoplankton Ecology group (SOPhyE) at the Bedford Institute of Oceanography, reported in Devred et al. (2025). Measured in situ NPP reflects the NPP integrated rates (from ^{13}C incubations) measured during the BELAS-1 expedition (see Fig. 3). Satellite NPP reflects integrated NPP down to the depth of 1% surface photosynthetic active radiation, while measured in situ NPP reflects integrated NPP down to the base of the primary production zone (Owens et al., 2015).

References

Ceballos-Romero, E., De Soto, F., Le Moigne, F. A. C., García-Tenorio, R., and Villa-Alfageme, M.: ^{234}Th-derived particle fluxes and seasonal variability: when is the SS assumption reliable? Insights from a novel approach for carbon flux simulation, Geophys. Res. Lett., https://doi.org/10.1029/2018GL079968, 2018.

Devred, E., Clay, S., Ringuette, M., Perry, T., Amirian, M., Irwin, A., and Finkel, Z.: Net primary production in the Labrador Sea between 2014 and 2022 derived from ocean colour remote sensing based on ecological regimes, Remote Sens. Environ., 323, 114713, https://doi.org/10.1016/J.RSE.2025.114713, 2025.

Owens, S. A., Pike, S., and Buesseler, K. O.: Thorium-234 as a tracer of particle dynamics and upper ocean export in the Atlantic Ocean, Deep Sea Res. Part II Top. Stud. Oceanogr., 116, 42–59, https://doi.org/10.1016/j.dsr2.2014.11.010, 2015.